Electronic Supplementary Material (ESI) for New Journal of Chemistry.

Supporting Information

Face-on-Oriented Formation of Bis(diimino)metal Coordination Nanosheets on Gold Electrodes by Electrochemical Oxidation

Hiroaki Maeda,*[a] Kenji Takada, [a] Naoya Fukui, [a] Hiroyasu Masunaga, [b] Sono Sasaki, [c, d] Kazuhito Tsukagoshi, [e] Hiroshi Nishihara *[a, f]

[a]Research Institute for Science and Technology, Tokyo University of Science, 2641 Yamazaki, Noda, Chiba, 278-8510, Japan.

[b]Japan Synchrotron Radiation Research Institute (JASRI), 1-1-1 Kouto, Sayo-cho, Sayo-gun, Hyogo 679-5198, Japan.

[c]Faculty of Fiber Science and Engineering, Kyoto Institute of Technology, Matsugasaki, Sakyo-ku, Kyoto 606-8585, Japan.

[d]RIKEN SPring-8 Center, 1-1-1 Kouto, Sayo-cho, Sayo-gun, Hyogo, 679-5148, Japan.

[e]Research Centre for Materials Nanoarchitectonics (MANA), National Institute for Materials Science (NIMS), Tsukuba, Ibaraki 305-0044, Japan

[f]Graduate School of Science and Technology, Tokyo University of Science, 2641 Yamazaki, Noda, Chiba, 278-8510, Japan.

E-mail: h-maeda@rs.tus.ac.jp (H. Maeda), nisihara@rs.tus.ac.jp (H. Nishihara)

Experimental

Materials

Hexaaminobenzene trihydrochloride (HAB·3HCl) was synthesized according to the literature [S1, S2]. Chemical reagents and organic solvents were purchased from commercial sources (TCI, FUJIFILM Wako Pure Chemicals, ALDRICH) and used without further purification. Water was purified by an Autopure WD500 (Yamato Scientific). Au/glass substrates (ca. 30 nm gold layer deposited on glass substrates) were purchased from Kenis Co. Ltd. The root means square (RMS) surface roughness of the Au/glass substrates was evaluated as 0.64-1.0 nm according to the roughness analysis by AFM measurement (Fig. S10a, c) and the Au(111) plane directs to the out-of-plane direction as shown in the X-ray scattering pattern of the bare Au/glass substrate (Fig. S1).

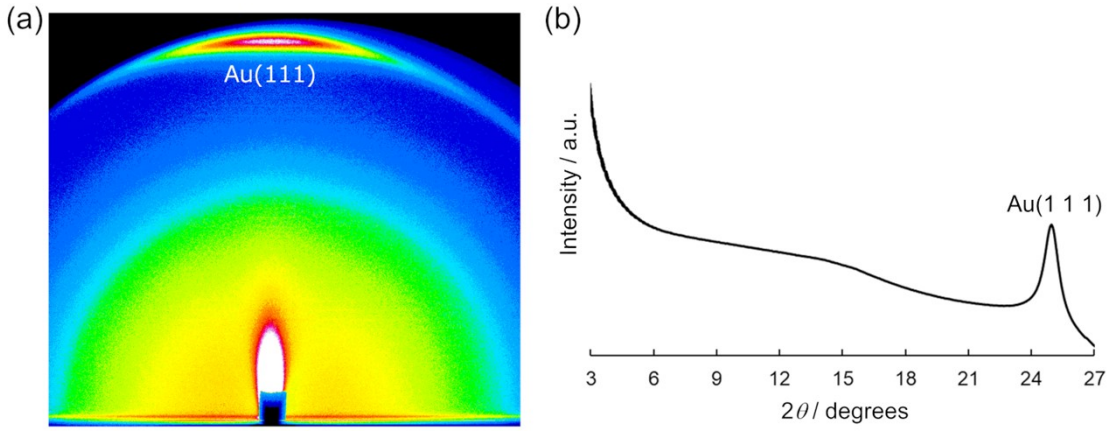

Fig. S1. (a) Two-dimensional scattering image obtained by GIXS and (b) diffraction pattern converted from the scattering image of the bare Au/glass substrate.

Apparatus

AFM topography images were obtained using an Agilent Technologies 5500 scanning probe microscope with an NCH silicon cantilever (NanoWorld) in the tapping mode, a Hitachi AFM5000II with an SI-DF40P2 cantilever in the DFM mode, or a NaioAFM with a PPP-NCLR prober in the phase imaging mode. Raman spectra were collected using an NRS-5500 (JASCO) with a 532-nm excitation laser. X-ray photoelectron spectra were collected using VersaProbeIII (ULVAC-PHI) with a monochromatic Al Kα X-ray source. The binding energy values in the spectra were standardized using an Au $4f_{7/2}$ peak at 84.0 eV. Grading incident X-ray scattering (GIXS) measurements were conducted using synchrotron radiation at Beamline BL05XU (λ = 1.0 Å) in Super Photon ring-8 (SPring-8). Electrochemical oxidation synthesis of MHABs was performed at room temperature in an Ar-purged glove box with an ALS 650DT electrochemical analyzer. An Ag/AgCl (sat. KCl aq.) and a Pt coil were used as a reference and a counter electrode, respectively. An Au/glass (Kenis) or an Au/mica was used as a working electrode. Cyclic voltammetry measurements of MHAB-modified Au/glass substrates were conducted at room temperature in a 1 M $^{n}Bu_4NPF_6/CH_3CN$ electrolyte solution degassed with

Ar. An $Ag/AgClO_4$ reference electrode (an Ag wire immersed in a 10 mM $AgClO_4$/0.1 M $^nBu_4NClO_4/CH_3CN$ solution), a Pt wire as a counter electrode, and an MHAB-modified Au/glass as a working electrode were connected to an ALS 750E electrochemical analyzer. The recorded potentials were calibrated using the redox potential of ferrocenium/ferrocene (Fc^+/Fc) in the same electrolyte solution.

Electrochemical oxidation synthesis of NiHAB-A and NiHAB-B

$Ni(OAc)_2 \cdot 4H_2O$ (1.5 mg, 6 μmol), HAB·3HCl (1.1 mg, 4 μmol), and $NaBF_4$ (55 mg) were dissolved in 5 mL of a diluted NH_3 aqueous solution (conc. NH_3 aq./H_2O = 1:5, ca. 2.3 M) in an Ar-purged glove box to prepare an electrolyte solution for the electrochemical oxidation synthesis. An Ag/AgCl reference, a Pt wire, and an Au electrode were immersed in the solution, and then an oxidation potential (+0.58 V or −0.10 V vs. Ag/AgCl) was applied for 180 s to form NiHAB on the working electrode surface. The modified electrodes were rinsed with water, removed from the glove box, and dried under the vacuum.

Electrochemical oxidation synthesis of NiHAB-C, NiHAB-D, and NiHAB-E

$Ni(OAc)_2 \cdot 4H_2O$ (1.5 mg, 6 μmol), HAB·3HCl (1.1 mg, 4 μmol), and $NaBF_4$ (55 mg) were dissolved in 5 mL of water, then a required amount of base was added to the solution (conc. NH_3 aq.: 33 μL, triethylamine (TEA): 70 μL, or ethylenediamine (EDA): 33 μL). An Ag/AgCl reference, a Pt wire, and an Au electrode were immersed in the solution, and then the potential of −0.10 V vs. Ag/AgCl was applied for 180 s to form NiHAB on the working electrode surface. The modified electrodes were rinsed with water, removed from the glove box, and dried under the vacuum.

Electrochemical oxidation synthesis of NiHAB-F and NiHAB-G

$Ni(OAc)_2 \cdot 4H_2O$ (1.5 mg, 6 μmol), HAB·3HCl (1.1 mg, 4 μmol) were dissolved in 50 mL of an NH_3 aqueous solution with a required concentration (2.3 M for NiHAB-F and 0.1 M for NiHAB-G), then 5 mL of the solution was added to $NaBF_4$ (55 mg). An Ag/AgCl reference, a Pt wire, and an Au electrode were immersed in the solution, and then the potential of −0.10 V vs. Ag/AgCl was applied for 180 s to form NiHAB on the working electrode surface. The modified electrodes were rinsed with water, removed from the glove box, and dried under the vacuum.

Electrochemical oxidation synthesis of CoHAB-A and CoHAB-B

$Co(OAc)_2 \cdot 4H_2O$ (1.5 mg, 6 μmol), HAB·3HCl (1.1 mg, 4 μmol), and $NaBF_4$ (55 mg) were dissolved in 5 mL of a diluted NH_3 aqueous solution (conc. NH_3 aq./H_2O = 1:5, ca. 2.3 M) in an Ar-purged glove box to prepare an electrolyte solution for the electrochemical oxidation synthesis. An Ag/AgCl reference, a Pt wire, and an Au electrode were immersed in the solution, and then an oxidation potential (+0.21 V or −0.10 V vs. Ag/AgCl) was applied for 180 s to form CoHAB on the working electrode surface. The modified electrodes were rinsed with water, removed from the glove box, and dried under the vacuum.

Electrochemical oxidation synthesis of CuHAB-B and CuHAB-F

For the preparation of CuHAB-B, $Cu(OAc)_2 \cdot H_2O$ (1.1 mg, 6 μmol), HAB·3HCl (1.1 mg, 4 μmol), and $NaBF_4$ (55 mg) were dissolved in 5 mL of a diluted NH_3 aqueous solution (conc. NH_3 aq./H_2O = 1:5, ca. 2.3 M) in an Ar-purged glove box to prepare an electrolyte solution. For the synthesis of CuHAB-F, $Cu(OAc)_2 \cdot H_2O$ (1.1 mg, 6 μmol), HAB·3HCl (1.1 mg, 4 μmol) were dissolved in 50 mL of a 2.3 M NH_3 aqueous solution, then 5 mL of the solution was added to $NaBF_4$ (55 mg). An Ag/AgCl reference, a Pt wire, and an Au electrode were immersed in the solution, and then the potential of −0.20 V vs. Ag/AgCl was applied for 180 s to form CuHAB on the working electrode surface. The modified electrodes were rinsed with water, removed from the glove box, and dried under the vacuum.

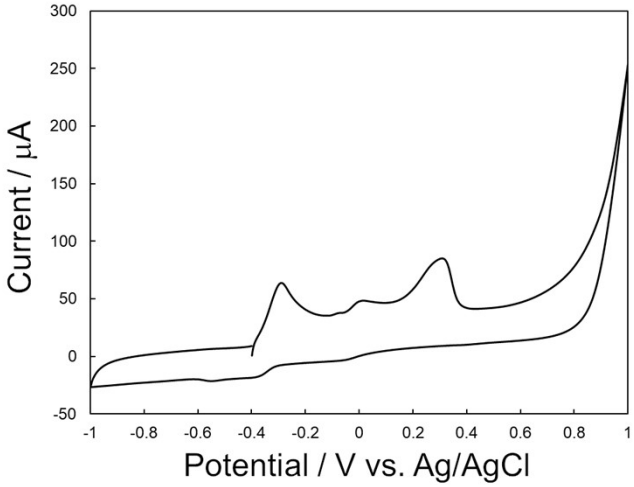

Fig. S2. Cyclic voltammogram of an electrolyte solution for NiHAB synthesis by the electrochemical oxidation method at a scan rate of 100 mV s^{-1}.

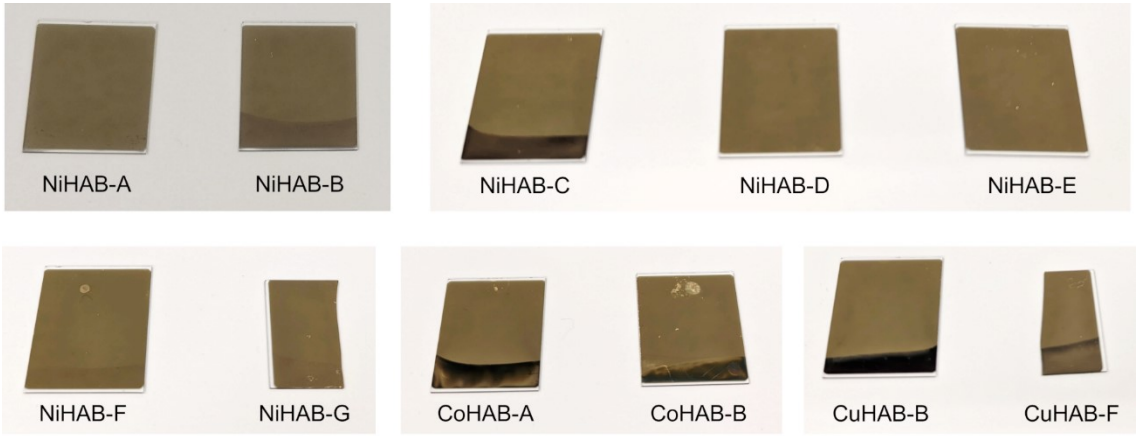

Fig. S3. Photographs of modified Au electrodes. The electrode size is 22 mm × 26 mm or ca. 13 mm × 22 mm.

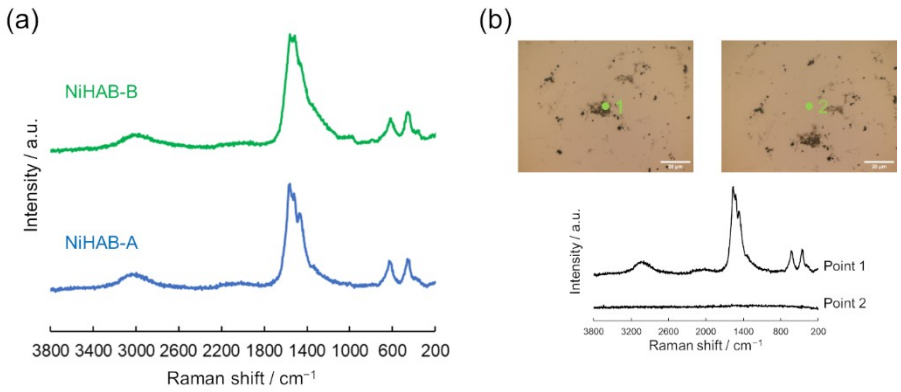

Fig. S4. (a) Raman spectra of NiHAB-A (blue solid line) and NiHAB-B (green solid line). (b) Optical microscopy images and corresponding Raman spectra of NiHAB-A at the points shown as green dots.

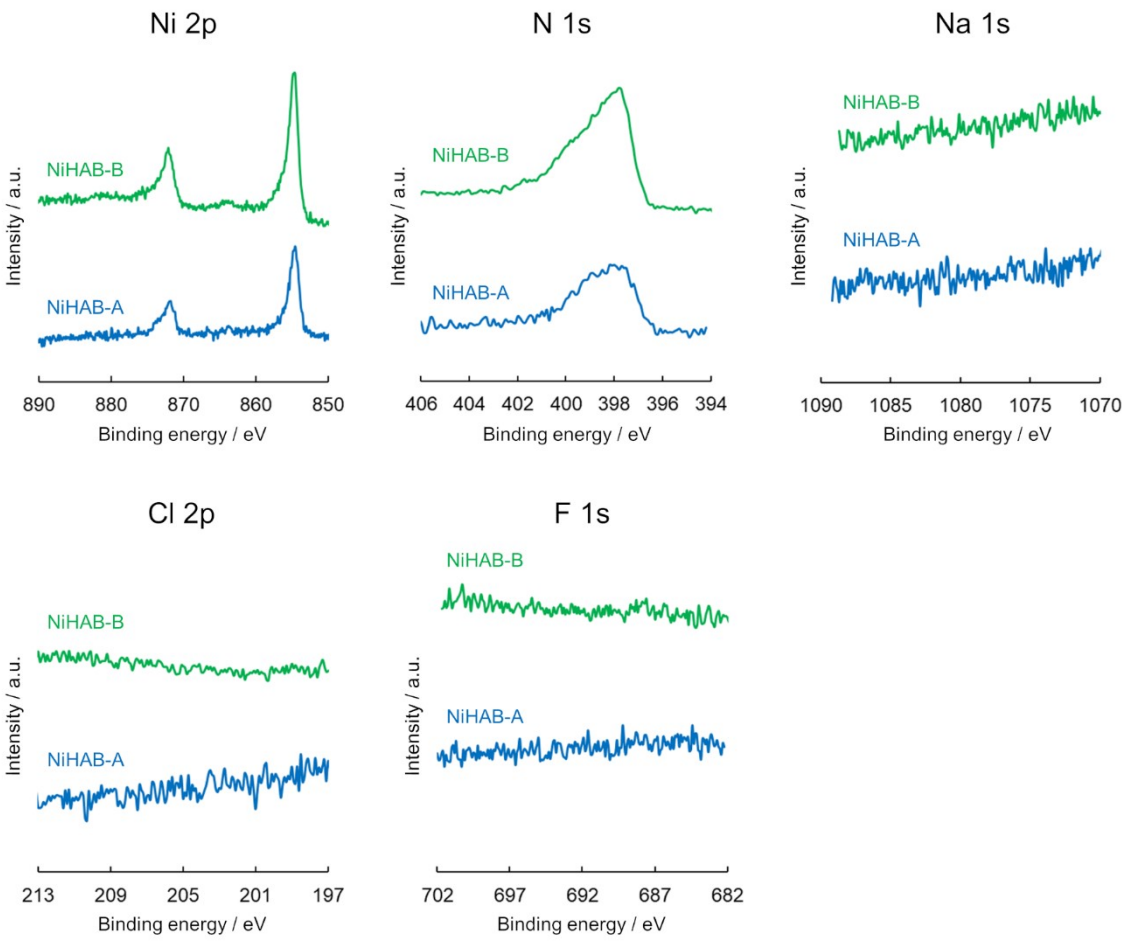

Fig. S5. XP spectra of NiHAB-A (blue solid line) and NiHAB-B (green solid line).

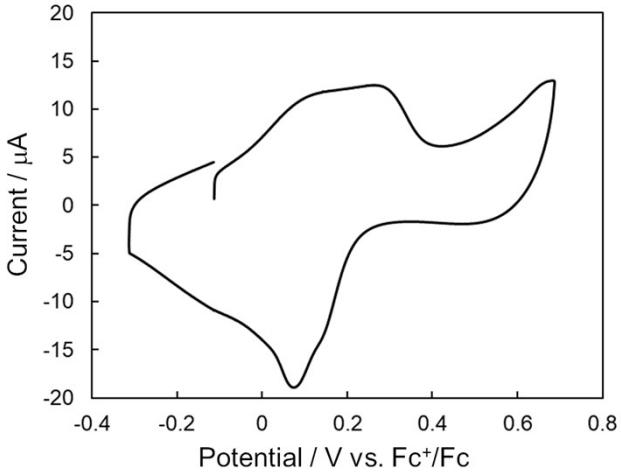

Fig. S6. Cyclic voltammogram of NiHAB-B in the steady-state recorded in a 1 M $^{n}Bu_4NPF_6/CH_3CN$ at a scan rate of 10 mV s^{-1}.

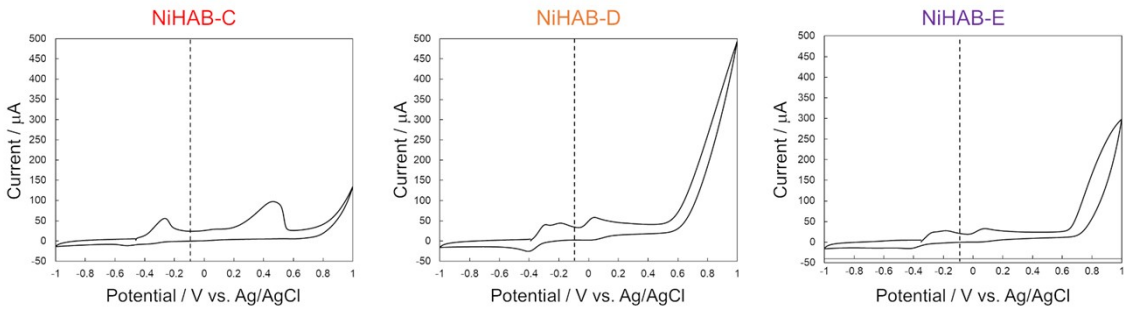

Fig. S7. Cyclic voltammograms of electrolyte solutions for the syntheses of NiHAB-C, NiHAB-D, and NiHAB-E. Dashed lines indicate the applied potential for NiHAB synthesis (−0.10 V vs. Ag/AgCl).

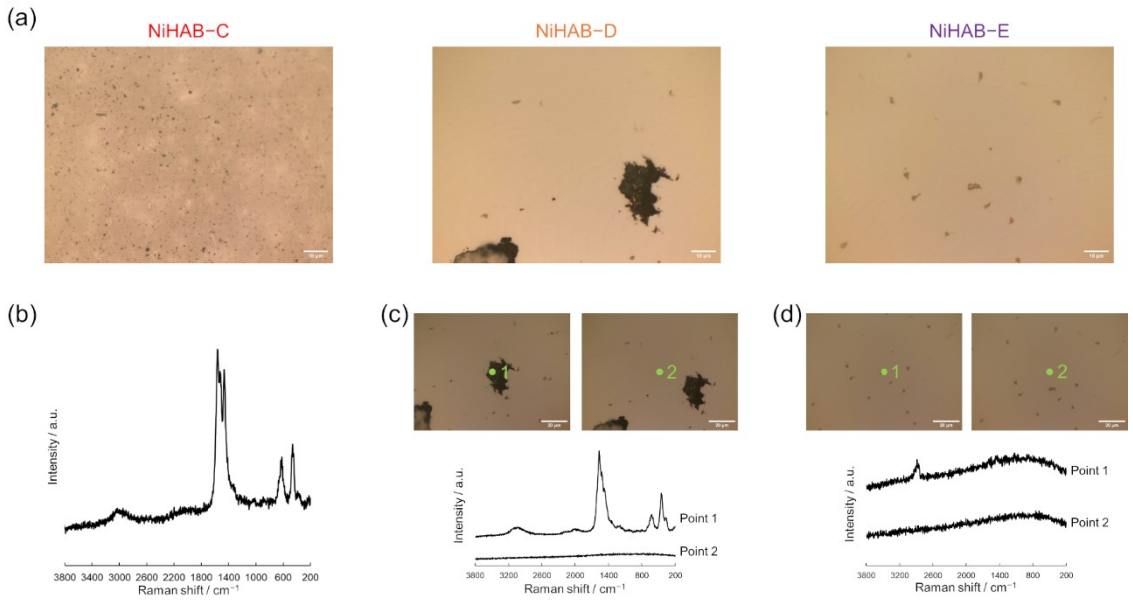

Fig. S8. (a) Optical microscopy images of NiHAB-C, NiHAB-D, and NiHAB-E. (b) Raman spectrum of NiHAB-C. Optical microscopy images and corresponding Raman spectra of (c) NiHAB-D and (d) NiHAB-E at the points shown as green dots.

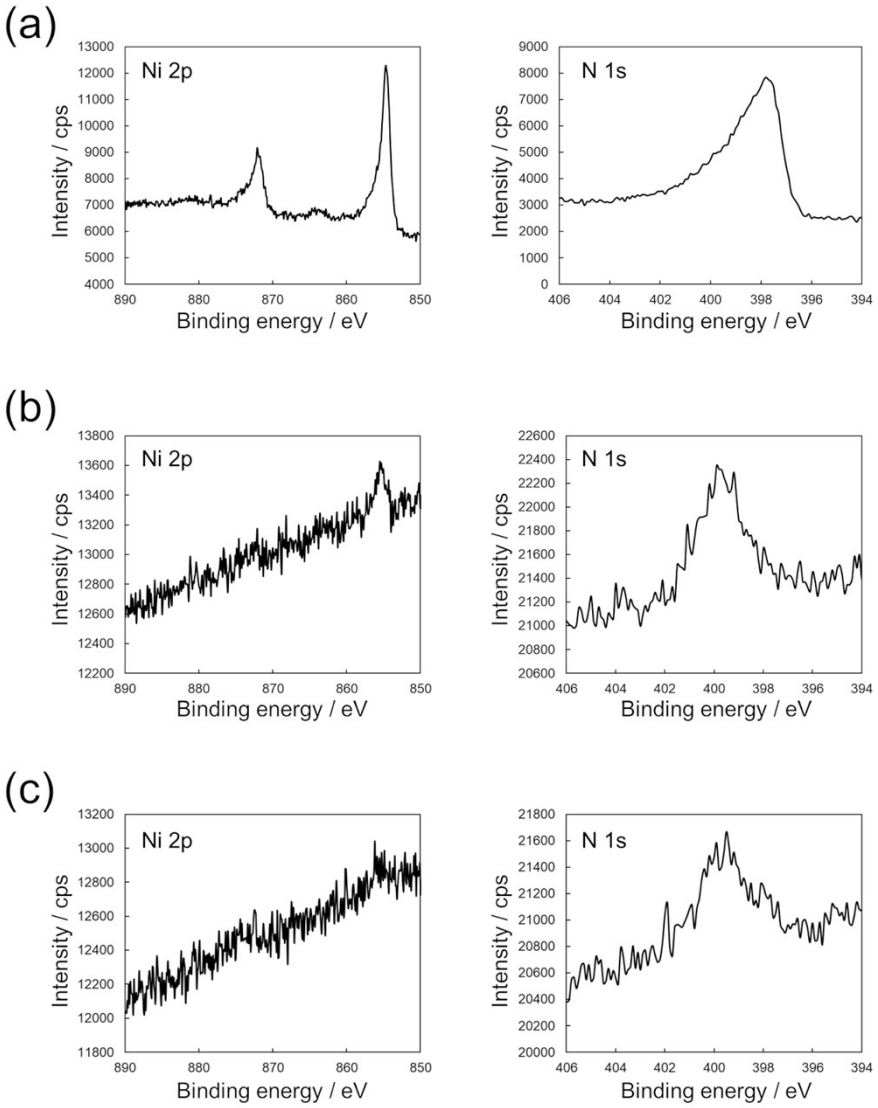

Fig. S9. XP spectra of (a) NiHAB-C, (b) NiHAB-D, and (c) NiHAB-E.

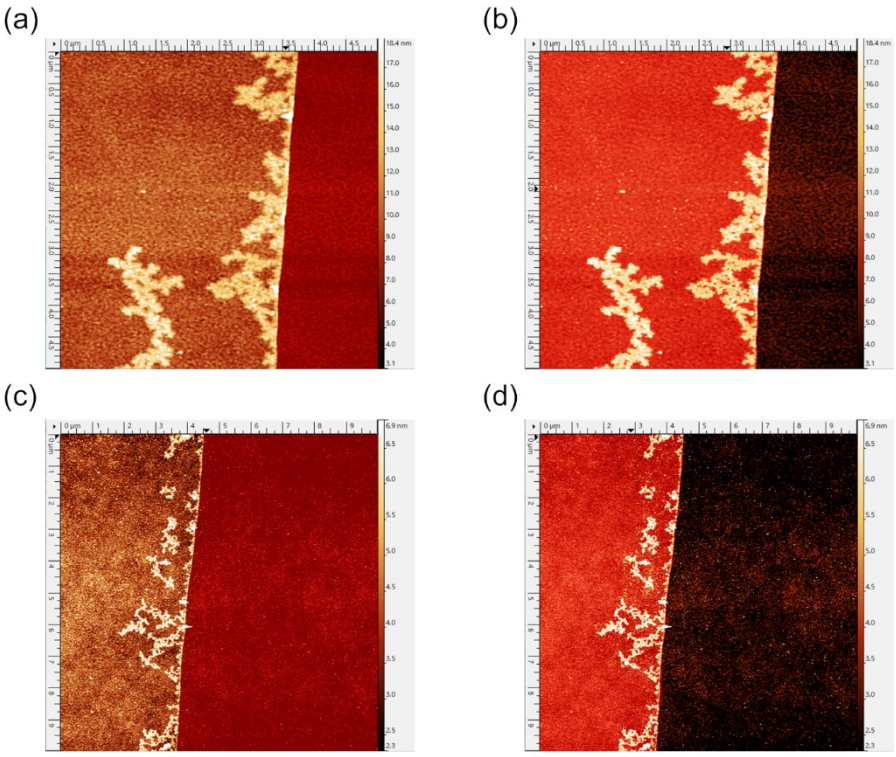

Area	RMS / nm
(a)	1.0
(b)	1.1
(c)	0.64
(d)	0.70

Fig. S10. Roughness analyses of (a) Au/glass area and (b) NiHAB-modified area of NiHAB-F and (c) Au/glass area and (d) NiHAB-modified area of NiHAB-G. The red-colored areas were used for roughness calculations.

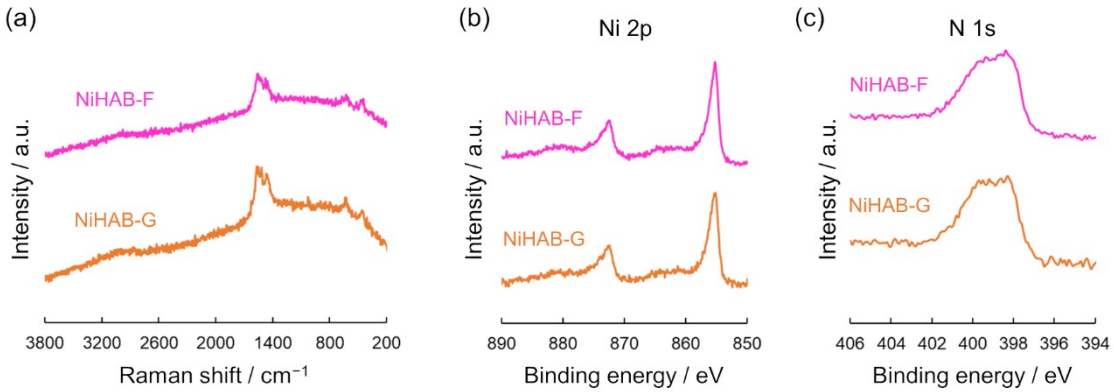

Fig. S11. (a) Raman spectra and XP spectra of (b) Ni 2p and (c) N 1s regions of NiHAB-F (pink solid line) and NiHAB-G (orange solid line).

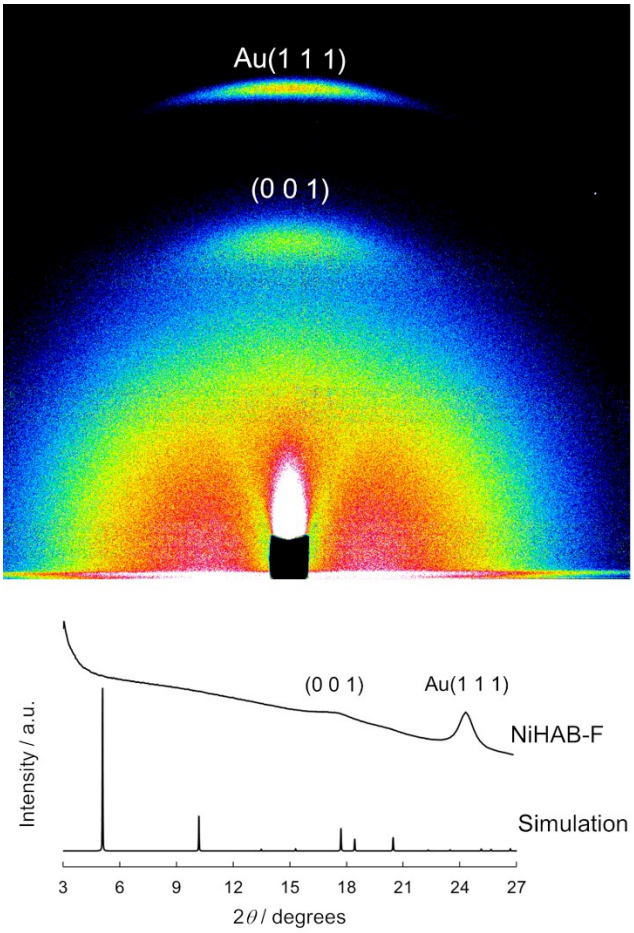

Fig. S12. Two-dimensional scattering image and diffraction pattern of NiHAB-F.

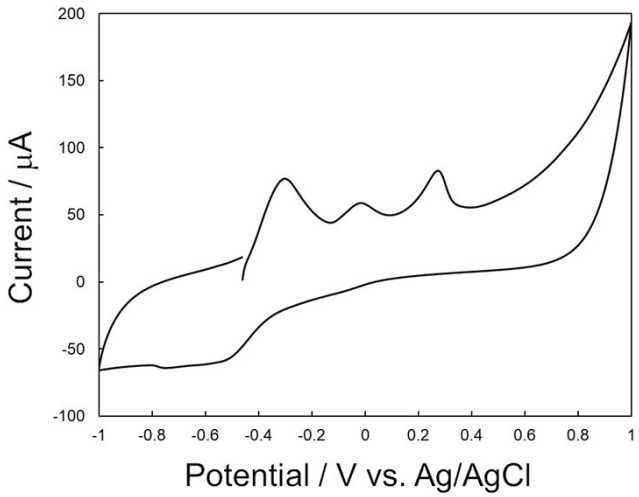

Fig. S13. Cyclic voltammogram of an electrolyte solution for CoHAB synthesis by the electrochemical oxidation method at a scan rate of 100 mV s^{-1}.

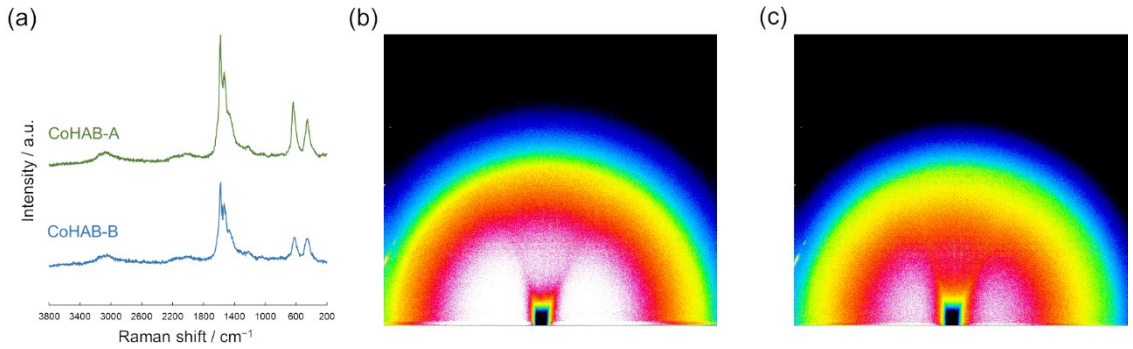

Fig. S14. (a) Raman spectra of CoHAB-A and CoHAB-B. Two-dimensional X-ray scattering patterns of (b) CoHAB-A and (c) CoHAB-B.

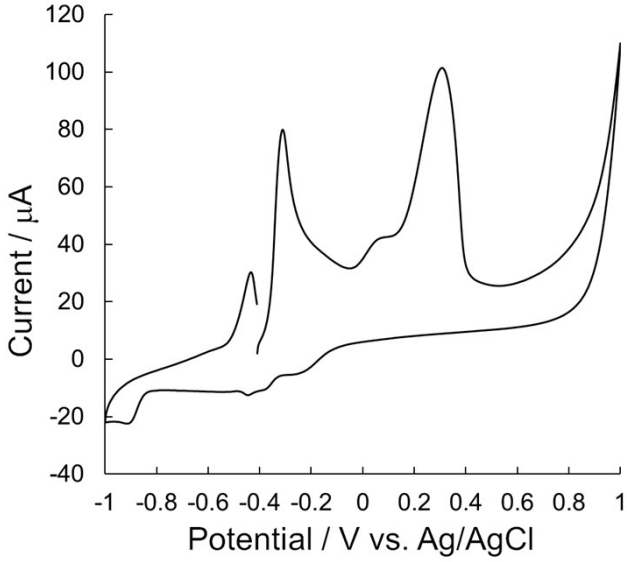

Fig. S15. Cyclic voltammogram of an electrolyte solution for CuHAB synthesis by the electrochemical oxidation method at a scan rate of 100 mV s^{-1}.

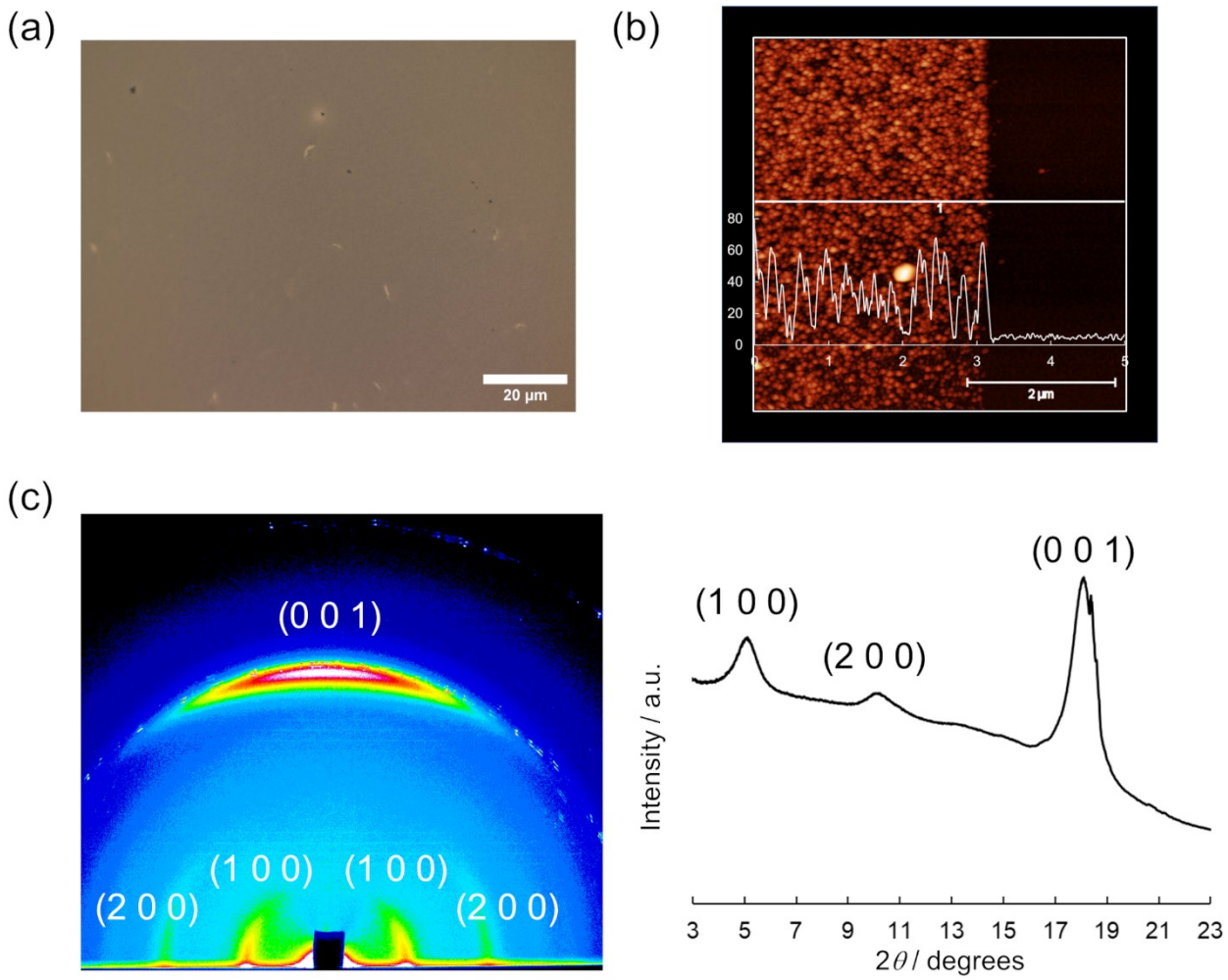

Fig. S16. (a) Optical microscopic image, (b) AFM topography image (inset: height profile at the white line), (c) two-dimensional X-ray scattering pattern and converted diffraction pattern of CuHAB-B.

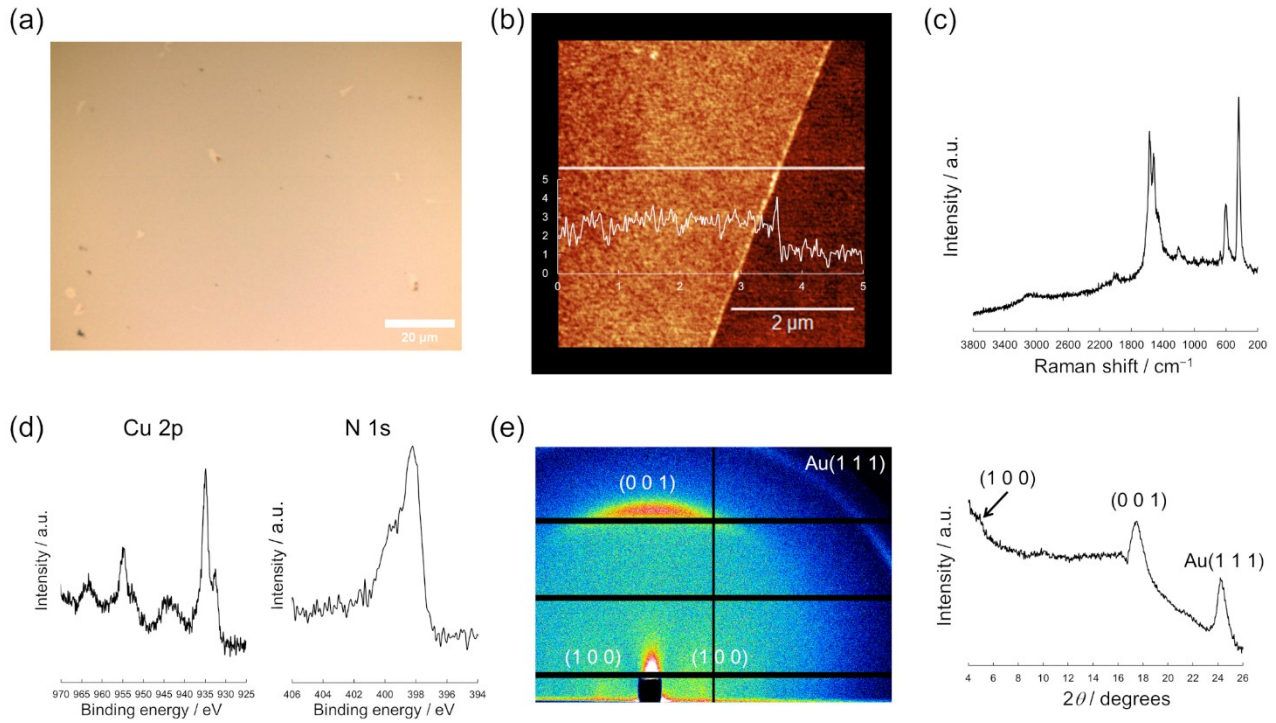

Fig. S17. (a) Optical microscope image, (b) AFM topography image (inset: height profile at the corresponding white line), Raman spectrum, (d) XP spectra, (e) two-dimensional X-ray scattering pattern, and converted diffraction pattern of CuHAB-F.

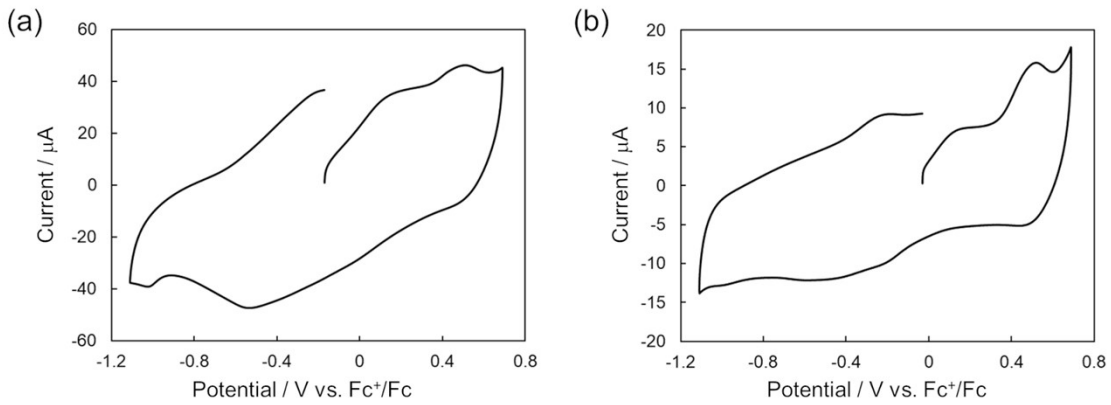

Fig. S18. Cyclic voltammograms of (a) CoHAB-B and (b) CuHAB-F in the steady-state recorded in a 1 M $^{n}Bu_4NPF_6/CH_3CN$ at a scan rate of 50 mV s^{-1}.

References

S1 Z.-G. Tao, X. Zhao, X.-K. Jiang and Z.-T. Li. *Tetrahedron Lett.* 2012, **53**, 1840.

S2 J. Mahmood, D. Kim, I.-Y. Jeon, M. S. Lah and J.-B. Baek. *Synlett* 2013, **24**, 246.